

# GDOP Classification and Approximation by Implementation of Time Delay Neural Network Method for Low-Cost GPS Receivers

M. H. Refan<sup>\*(C.A.)</sup> and A. Dameshghi\*

**Abstract:** Geometric Dilution of Precision (GDOP) is a coefficient for constellations of Global Positioning System (GPS) satellites. These satellites are organized geometrically. Traditionally, GPS GDOP computation is based on the inversion matrix with complicated measurement equations. A new strategy for calculation of GPS GDOP is construction of time series problem; it employs machine learning and artificial intelligence methods for problem-solving. In this paper, the Time Delay Neural Network (TDNN) is introduced to the GPS satellite DOP classification. The TDNN has a memory for archiving past event that is critical in GDOP approximation. The TDNN approach is evaluated all subsets of satellites with the less computational burden. Therefore, the use of the inverse matrix method is not required. The proposed approach is conducted for approximation or classification of the GDOP. The experiments show that the approximate total RMS error of TDNN is less than 0.00022 and total performance of satellite classification is 99.48%.

**Keywords:** GDOP, GPS, Approximation, Classification, TDNN.

## 1 Introduction

THE satellite-based navigation system is conducted based on the Global Positioning System (GPS). This system is based on radio communication which broadcasts precise timing signals. GPS user's location is determined on the Earth based on radio signals [1]. The number of GPS satellites in space is 24, it is designed based on signal transmission by 2 frequency carrier waves and 2 sets random telegraphic codes (C/A code and P-code) [2, 3]. The Geometric Dilution of Precision (GDOP) is relationship between measurement error and position determination error; it is a factor that describes the effect of geometry on between satellites [4, 5]. Therefore, it is sometimes necessary to select the satellite subset that offers the best or most acceptable solution [6]. The common method for calculating GDOP is matrix inversion, this method is

designed based on all combinations and select the minimum one [7]. However, this process can guarantee to achieve the optimal subset, but the computational complexity is usually too intensive to be practical [8]. In [9, 10], the fundamentals of GPS GDOP are described. In [8] a method is presented thorough of the GPS GDOP metric and the associated bounds of GDOP based on formal linear algebra. Artificial Neural Networks (ANNs) is employed to rephrase the problem as function approximation [11]. The approximation problem is conducted based on a variety of ANN-based methods [12, 13]. The Support Vector Regression (SVR) method is another approximation strategy for GSP GDOP calculation [14]. Genetic Programming (GP) is used for GDOP approximation in [15]. In [16], backpropagation training algorithms is used for classification of GPS satellites. In [18], a new method is proposed based on novel NN for GPS GDOP classification; it used a neuro-fuzzy inference system for approximation. In [19], a new method based on GA is proposed for GDOP analysis; in this paper for proper selection of satellite a hybrid method for approximation of GDOP using optimum number of satellites based on popular optimization technique is introduced. In another paper [20], a GA method is used for optimal satellite

Iranian Journal of Electrical and Electronic Engineering, 2020.

Paper first received 19 October 2018, revised 13 August 2019, and accepted 25 August 2019.

\* The authors are with the Department of Electrical Engineering, Shahid Rajaei Teacher Training University, Lavizan, Tehran, Iran.

E-mails: [refan@sru.ac.ir](mailto:refan@sru.ac.ir) and [a.dameshghi@sru.ac.ir](mailto:a.dameshghi@sru.ac.ir).

Corresponding Author: M. H. Refan.

selection for GPS navigation. The weighted GDOP is introduced in [21] for applications of multi-GNSS (global navigation satellite system) constellations. A satellite selection algorithm based on Particle Swarm Optimization (PSO) is proposed in [22]. A fast satellite selection algorithm is proposed in [23], this method is based on floating high cut-off elevation angle based on ambiguity dilution of precision (ADOP) for instantaneous multi-GNSS single-frequency relative positioning.

In this paper, the Time Delay Neural Network (TDNN) method is used to reduce the computational complexity and speed up of the computation. The small training time is one of the best features of this approach in comparison to the other forms of NNs. The TDNN method requires a small number of computations for output calculation [18]. In this paper, TDNN is utilized to GDOP approximation and classification.

The TDNN is a type of recurrent neural networks (RNNs) [24, 25]. The RNN architecture presented in these papers utilizes a time-window of past values of a given time-series for one-step and multi-step ahead approximations.

The main innovation of the article is as follows:

1. One of the innovations is the use of a Time Delay Neural Network (TDNN) instead of the multilayered perceptron (MLP), which is better adapted to the dynamics of the system.
2. The proposed method is implemented on an actual navigation simulator.

The remained of the paper is organized as follows. In Section 2, a brief review of GPS GDOP computation is discussed. TDNN method is discussed in Section 3. Section 4 shows the experimental setup and implementation procedure. The experimental result is presented in Section 5, and finally, our study is concluded in Section 6.

## 2 GDOP

A simple interpretation of how much one unit of measurement error contributes to the derived position solution error is derived based on GPS GDOP factor. Four satellites for user position determination is the requirement of GPS. Fig. 1 is satellite geometry representation, based on this figure good satellite geometry is obtained if the four satellites spread apart; in this condition, GDOP is minimum value. The effect of satellite geometry is measured by a GDOP figure.

The value of the GDOP is changed over the time based on relative motion of the satellites and the receiver(s). The azimuth angle is a factor for the best four-satellite selection. Elevation and azimuth of satellite according to (1) are involved in the calculation of GDOP factor [12-14].

$$G = \begin{bmatrix} \cos(E1) \times \sin(AZ1) & \cos(E1) \times \cos(AZ1) & \sin(E1) & 1 \\ \cos(E2) \times \sin(AZ2) & \cos(E2) \times \cos(AZ2) & \sin(E2) & 1 \\ \cos(E3) \times \sin(AZ3) & \cos(E3) \times \cos(AZ3) & \sin(E3) & 1 \\ \cos(E4) \times \sin(AZ4) & \cos(E4) \times \cos(AZ4) & \sin(E4) & 1 \end{bmatrix} \quad (1)$$

The GDOP factor is (2):

$$GDOP = \sqrt{\text{trace}(G^T G)^{-1}} = \sqrt{\frac{\text{trace}[\text{adj}(G^T G)]}{\det(G^T G)}} \quad (2)$$

where  $G^T G$  is a matrix with  $4 \times 4$  rank, the number of eigenvalues if this matrix is four,  $\lambda_i$  ( $i = 1, 2, 3, 4$ ). The representation for four eigenvalues is based on  $\lambda_i^{-1}$ . Based on the fact that the trace of a matrix is equal to the sum of its eigenvalues (2), it can be represented as (3):

$$GDOP = \sqrt{\lambda_1^{-1} + \lambda_2^{-1} + \lambda_3^{-1} + \lambda_4^{-1}} \quad (3)$$

The mapping is performed by defining the four variables.

$$f_1(\bar{\lambda}) = \lambda_1 + \lambda_2 + \lambda_3 + \lambda_4 = \text{trace}(G^T G) \quad (4)$$

$$f_2(\bar{\lambda}) = \lambda_1^2 + \lambda_2^2 + \lambda_3^2 + \lambda_4^2 = \text{trace}[(G^T G)^2] \quad (5)$$

$$f_3(\bar{\lambda}) = \lambda_1^3 + \lambda_2^3 + \lambda_3^3 + \lambda_4^3 = \text{trace}[(G^T G)^3] \quad (6)$$

$$f_4(\bar{\lambda}) = \lambda_1 \lambda_2 \lambda_3 \lambda_4 = \det(G^T G) \quad (7)$$

The  $\lambda^{-1}$  can be viewed as a functional  $R^4 \rightarrow R^4$  mapping  $G$  to  $\lambda^{-1}$  (Type 1).

$$(x_1, x_2, x_3, x_4)^T = (f_1, f_2, f_3, f_4)^T \quad (8)$$

$$(y_1, y_2, y_3, y_4)^T = (\lambda_1^{-1} + \lambda_2^{-1} + \lambda_3^{-1} + \lambda_4^{-1})^T \quad (9)$$

The GDOP can be viewed as a functional  $R^4 \rightarrow R^1$  mapping from  $\bar{G}$  to GDOP (Type 2).

$$(x_1, x_2, x_3, x_4)^T = (f_1, f_2, f_3, f_4)^T \quad (10)$$

$$y = GDOP \quad (11)$$

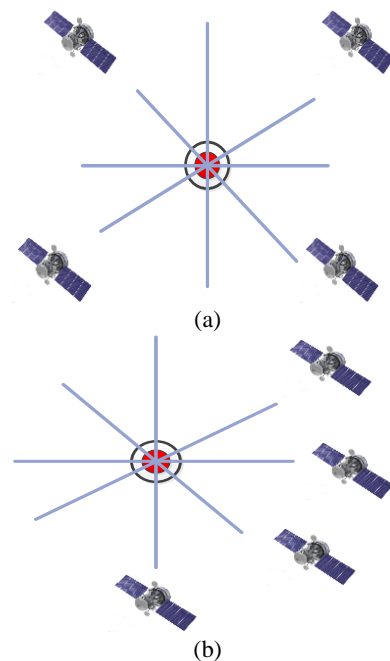


Fig. 1 Satellite geometry representation; a) Good DOP and b) Poor DOP.

### 3 Theory of TDNN

The weakness of the Feed Forward Neural Networks (FFNNs) is lack of memory; memory helps to create a communication map between input behaviors and output behaviors. In this paper, a TDNN is utilized for approximation and classification the GDOP. The utilized method is reduced structure of NARX-NN model. The NARX-NN and TDNN are based on RNNs [26, 27]. A type of RNN is NARX-NN. This network is used for modeling nonlinear systems. With a fixed step time, the proposed structure is such that the output is given as feedback to the input. The NAREX model is as (12).

$$y(n+1) = f \left[ x(n-d_x), \dots, x(n-1), x(n); y(n-d_y), \dots, y(n) \right] \quad (12)$$

where  $x(n)$  and  $y(n)$  are the input and output of the case study system at time step  $n$ ,  $d_x$  is input memory order and  $d_y$  is output memory order. The nonlinear mapping function show with  $f(\cdot)$ . The output of the NARX-NN is as (13).

$$y(n+1) = f_0 \left[ b_0 + \sum_{h=1}^{N_h} w_{h0} f_h(b_h + \sum_{i=0}^{d_x} w_{ih} x(n-i) + \sum_{j=0}^{d_y} w_{jh} y(n-j)) \right] \quad (13)$$

where  $w_{h0}$ ,  $w_{ih}$ , and  $w_{jh}$ ;  $i = 1, 2, \dots, d_x$ ;  $j = 1, 2, \dots, d_y$ ;  $h = 1, 2, \dots, N$  are the network weight vectors,  $b_h$  and  $b_0$  are the biases, the activation functions of the hidden and output layers are  $f_h$  and  $f_0$ , receptively. Fig. 2 is the structure of NARX NN. Based on this figure, NARX model have one input layer, one hidden layer and one output layer as three main layers. From this figure,  $x(n)$  and  $z^{-1}$  represents the unit time delay and external input, receptively. The NARX typical structure is based on a feedback connection from the output neuron. However, the NARX network is designed as a TDNN. For this goal, a reduced structure should be designed. The TDNN model is a feed-forward network without the delayed feedback loops [28]. A TDNN equation is as (14). In TDNN, (13) is reduces to (15).

$$y(n+1) = f \left[ x(n-d_x), \dots, x(n-1), x(n) \right] \quad (14)$$

$$y(n+1) = f_0 \left[ b_0 + \sum_{h=1}^{N_h} w_{h0} f_h \left( b_h + \sum_{i=0}^{d_x} w_{ih} x(n-i) \right) \right] \quad (15)$$

In the TDNN approximation model is based on past values of external input  $x(n)$ . In traditional RNNs in contrast proposed TDNN the previously input is used as the same time-series that prediction should be done for it. Fig. 3 is the structure of TDNN. This topology is a reduced structure from NARX-NN by eliminating the tapped delayed lines for the output time-series.

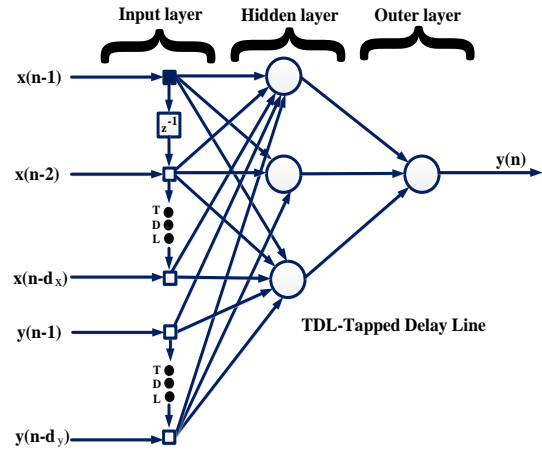


Fig. 2 The structure of NARX-NN.

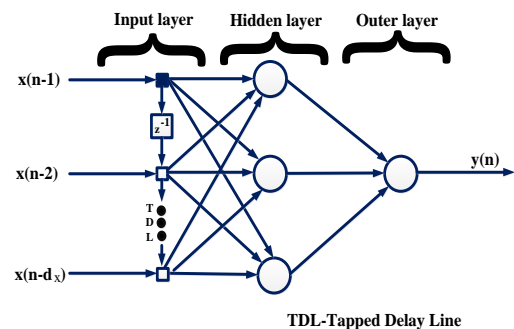


Fig. 3 The TDNN topology.

#### 3.1 Training of TDNN

Because of the similar structure of TDNN and multilayered perceptron (MLP), backpropagation can be applied to train the TDNN. The TDNN has three layers, including the input layer, hidden layer, and output layer. Back-propagation through time [29] is used to train the TDNN of this model. The performance index of the algorithm is

$$J = \sum_{k=0}^{\infty} \|e(k)\|^2 \quad (16)$$

where  $e(k)$  is the error between model output and training goal for each input at discrete time. Then, the chain rule of each error's gradient can be expressed as (17):

$$\frac{\partial J}{\partial \omega_{ij}^l} = \sum \frac{\partial J}{\partial y_j^{l+1}(k)} \cdot \frac{\partial y_j^{l+1}(k)}{\partial \omega_{ij}^l} \quad (17)$$

where  $\omega_{ij}^l$  is the weight of the neuron  $i$  in the  $l$ -th layer to the neuron  $j$  in the  $(l+1)$ -th layer.  $y_j^l$  the output of the neuron in the  $l$ -th layer. For the layers  $l: 1 \leq l \leq L-1$ .

$$\frac{\partial y_j^{l+1}(k)}{\partial x_j^l(k)} = \begin{cases} \omega(t-k), & 0 \leq t-k \leq T_l \\ 0, & \text{Other} \end{cases} \quad (18)$$

where  $x_j^l$  is the input of the neuron  $i$  in the  $l$ -th layer and

$\omega$  is a vector of the weight, whose length is  $T_l$ . From (16)–(18), (19) and (20) can be obtained as the weight algorithm used to train the TDNN, where

$$\omega_{ij}^l(k+1) = \omega_{ij}^l(k) - \eta \delta_j^{l+1}(k) x_i^l(k) \quad (19)$$

$$\delta_j^l(k) = \begin{cases} -2e(k) f' [y_j^l(k)], & l = L \\ f' [y_j^l(k)] \sum_{m=1}^{N_{l+1}} \Delta_m^{l+1}(k) \omega_{jm}^l, & 1 \leq l \leq L-1 \end{cases} \quad (20)$$

where  $\Delta_m^l(k) = [\delta_m^l(k) \delta_m^l(k+1) \dots \delta_m^l(k+T_{l-1})]$ ,  $\eta$  the coefficient used to adjust the step of BP algorithm, usually, it is between 0 and 1,  $x_i^l(k)$  is the input of the neuron  $i$  in the  $l$ -th layer and  $f()$  is the Sigmoid function used in the neuron.

#### 4 Experimental Setup and Implementation

The experimental setup and implementation structure of the proposed method is based on Fig. 4.

##### 4.1 Proposed Strategy for Implementation

The proposed strategy in this paper includes various blocks as described below.

- (a) The receivers are placed at the same point, which causes the sharing satellite of two receivers and calculations with the same inputs.
- (b) An antenna for the receiver that is for inverse

matrix calculation.

- (c) An antenna for the receiver that is used TDNN approximation and classification.
- (d) An experimental board to prepare the practical data.
- (e) Computer Number 1 for GDOP computing based on the inverse matrix. The input of this system (from receiver #1) includes elevation and azimuth of satellite according to (1). This information is provided on the basis of reading the binary protocol information.
- (f) Computer Number 2 for GDOP computing based on approximation and classification using the TDNN model. The input of this system (from receiver#2) is GDOP. This information is provided on the basis of reading the NMEA protocol information.
- (g) The block diagram of GPS GDOP clustering using TDNN. The GDOP classifier is employed for selecting one of the acceptable subsets.
- (h) The “h” subsection is for the two types of GDOP mappings, this topology is input-output communication based on TDNNs model. This map is nonlinear; this map cannot be solved analytically. The proposed NN approximates it easily and precisely.

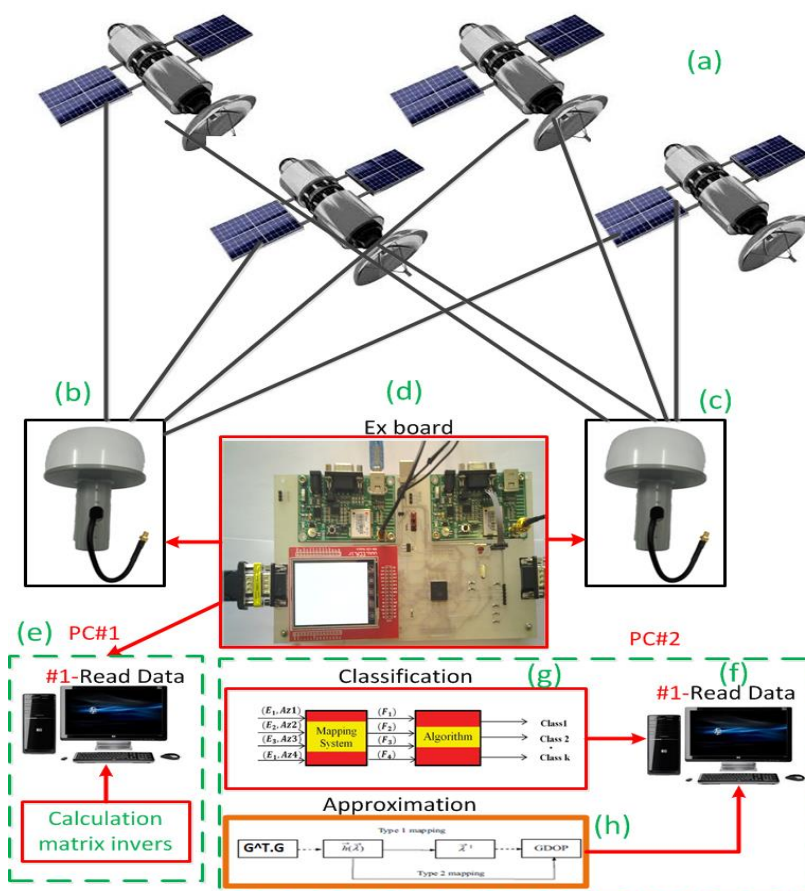


Fig. 4 Proposed strategy.



Fig. 5 Experimental hardware.

**4.2 Experimental Setup**

Fig. 5 shows the hardware test rig, this hardware is implemented for the experimental setup. The comparison of the accuracy inverse matrix method with the accuracy of the TDNN proposed method is conducted based on this experimental setup. The microcontroller of this setup is ARM 7X 256. This setup is programmed by a USB connection. This hardware is responsible for correcting and displaying the GDOP. Generally, the hardware is designed on a two-layer board and it has several modules and a microcontroller. Based on two separate antennas, the proposed setup uses two GPS receivers simultaneously. In this research, two low-cost GPS (LEA-6H) [29] receivers manufactured by U-Blox Company is used. The LEA-6H receiver is a single-board, fifty parallel-channels, L1-only coarse acquisition (C/A) code capability. This language protocol of receiver is a binary message, NMEA and RTCM. The LEA - 6H is tracked 16 satellites and is operated with single frequency. The selection of the satellites is a capability of this receiver that is used for the implementation of this paper proposed strategy.

**4.3 Setting of Proposed Structure**

The hardware to be located at the top of the building of the building of GPS Research Lab in Shahid Rajae Teacher Training University, which has the approximate position of  $(x_p = 3226206.85 \quad y_p = 4054570.66 \quad z_p = 3709308.89)$  m in WGS-84 ECEF coordinate. The GDOP is computed every 2 min by hardware and receiver. Simulation is conducted using a core i7 2.90 GHz computer. The MATLAB 2016a version software is used for the computer coding. In this paper, the TDNN model is utilized to perform the Type 1 and 2 mappings. The accuracy of the GDOP approximation models is evaluated by (21):

$$RMS = \sqrt{\frac{1}{M} \sum_{i=1}^M (x_i - x'_i)^2} \tag{21}$$

where  $x_i$  is the GDOP from direct matrix inversion and  $x'_i$  is output from the approximation function obtained from approximation methods,  $M$  is the number of test data. The GDOP approximation error is defined as (22):

$$E_{1,2} = GDOP_{matrix} - GDOP_{TDNN,GPS} \tag{22}$$

To evaluate the classification performance of the TDNN algorithm, the GDOP quality range must be clear. GDOP factor value rarely is close to 1. When this factor is much higher than 6 the positioning is impossible. Range  $0 < g \leq 2$  is excellent and GPS receiver shows more accurately positioning. Table 2 shows the GDOP ratings.

**5 Experimental Result**

**5.1 Evaluation of TDNN**

The GDOP calculation based on matrix inverse is

according to (2). The average value of GDOP for our GPS data is 2.354 and the run time is about 0.112 s. Fig. 6 is a represented of all satellites in view. Fig. 7. is the DOP as function time for all satellites.

The GDOP solution by matrix inversion shows with black point in Fig. 8. In this figure, the green point shows TDNN approximation performance (Type 1) and the red point is very close to the green point which means the excellent approximation performance for TDNN. Fig. 9 shows GDOP approximation error. The TDNNs have great approximation ability and suitability in GDOP estimation. In Fig. 10 the second map is used to approximate GDOP by TDNN. This figure shows GDOP approximation by TDNN (Type 2) and the purple point closes to the green point. The approximation error of this type is more concentrated around zero (Fig. 11). Results showed that, after approximation, the one-output architectures, provided better GDOP mapping accuracy than the four-output architectures. RMS error for TDNN (Type 2) is 0.002 that is less than the first type approximation error (Table 2). The results of Figs. 8 and 10 are obtained with 100 epoch and 4 neuron hidden layers.

**Table 1** Classification range of GDOP.

Class number	GDOP value	Rating
Class 1	$0 < g \leq 2$	Excellent
Class 2	$2 < g \leq 3$	Good
Class 3	$3 < g \leq 4$	Moderate
Class 4	$4 < g \leq 5$	Fair
Class 5	$> 5$	Poor

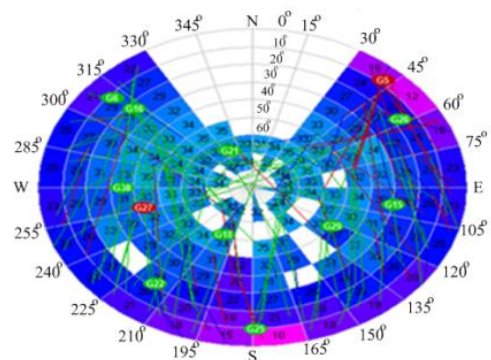


**Fig. 6** Sky plot in view of satellites.

**Table 2** Statistical measures of approximations error.

Parameters	RMS	MAX	MIN	AVE	VAR
E1 (Type1)	0.00029	1.1	0	0.025	0.126
E1 (Type 2)	0.00023	0.65	0	0.016	0.037
E2	0.00123	1.8	0.08	0.045	0.115

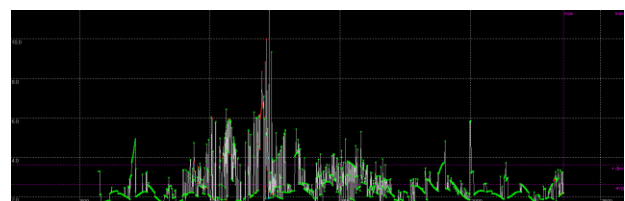


**Fig. 7** GDOP value.

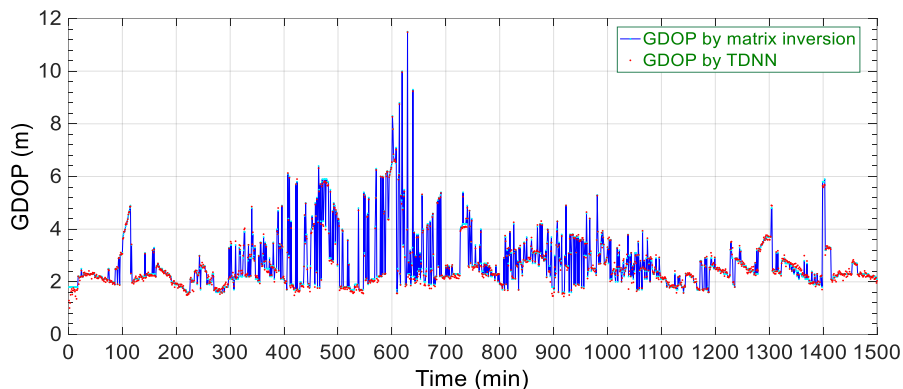


Fig. 8 GDOP approximated by TDNN (Type 1).

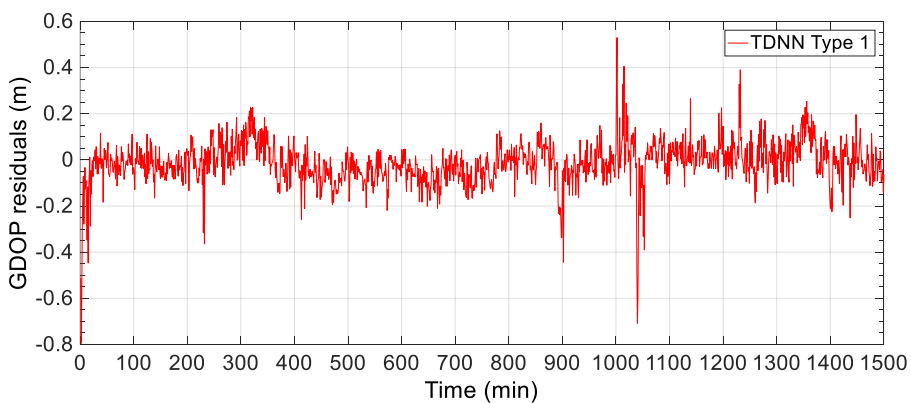


Fig. 9 GDOP approximation error (Type 1).

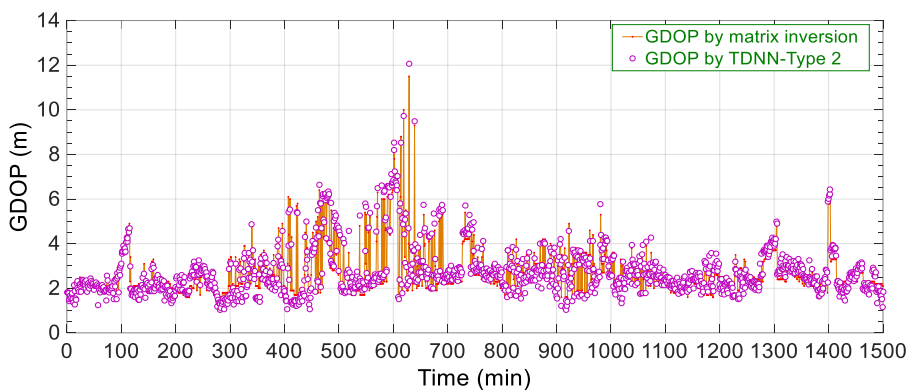


Fig. 10 GDOP approximated by TDNN (Type 2).

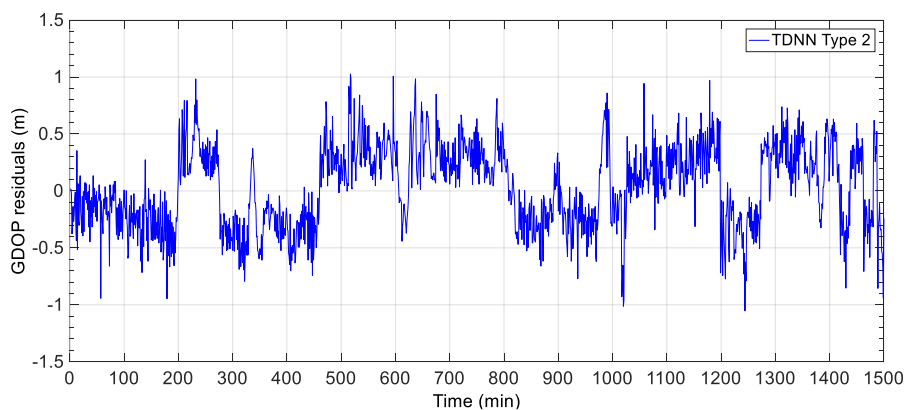


Fig. 11 GDOP approximation error (Type 2).

The  $E_2$  in Table 2 is the error between internal algorithms of GPS receiver with the output of the inverse matrix. It is clear that the proposed method has better accuracy than it. There must be a trade-off for the selection of training patterns. Increasing the number of hidden neurons and increasing the training patterns has some disadvantages, including high memory size for software implementation and time complexity for hardware implementation.

This paper 100 epochs with 4 neuron hidden layer is best in terms of accuracy and speed (tradeoff). The low training time for real-time operation is very important. Increasing the number of neurons or epochs increases the training time to minutes and hours, which is not suitable for positioning. The classification performances by TDNN are shown in histogram form (Fig. 12). This result is based on 3 neurons hidden layer and 50 epochs. As can be seen, the TDNN algorithm is successful in classification. In this algorithm, in fair and poor categories are 1.2% and 1.4% errors, respectively. Recognition present is given by (23):

$$\sum_{i=1}^m \frac{1}{m(1 - \text{error percent for any class})} \times 100 \quad (23)$$

The algorithm has a success rate of 99.48 percent. Table 3 and Fig. 12 show TDNN clustering results for GPS GDOP.

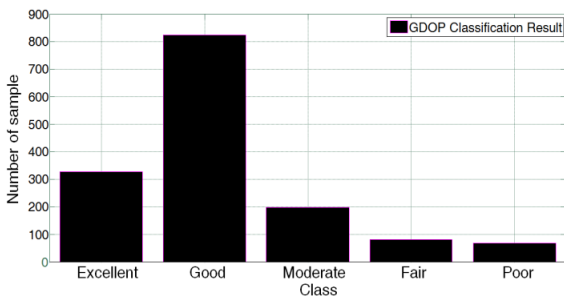


Fig. 12 GDOP classification result.

### 5.2 Compression

The results of GPS GDOP approximation using FFNN with BP are shown in Table 4. As it is shown the best result is obtained with 4 neurons in the hidden layer. In order to improve the accuracy, results are calculated after 10-50-100-150 epoch's training. Thus, increasing the hidden layer neurons number does not necessarily increase accuracy. Increasing the number of epoch's increases accuracy, but it increases the computational time that is not desirable. There must be a tradeoff between the accuracy and speed. The execution time (s) for different case shows in Table 4. The TDNN results are shown in Table 5. Based on different neuron numbers in the hidden layer and different epoch's, Table 5 shows the RMS error for GDOP approximation. Based on the new topology and improved structure of TDNN, the TDNN average error is less than FFBP. It is illustrated in this table that with four-neuron in hidden layer, result is best. The run time is reported in the last column of Table 5. Table 6 is compression TDNN method with [12, 14 15] in classification accuracy, the results of this table show that the proposed method is more or equal to other methods. Based on simulation results with a CORI7 (CPU), TDNN has the least time consuming compared to other methods.

Table 3 TDNN clustering results for GPS GDOP.

Cluster	1	2	3	4	5	Total	Err. [%]
Excellent	327	0	0	0	0	327	0
Good	0	824	0	0	0	824	0
Moderate	0	0	199	0	0	199	0
Fair	0	0	0	81	1	82	1.2
Poor	0	1	0	0	67	68	1.4

Table 4 FFNN-BP GDOP approximation results.

N. neuron	RMS	Time	RMS	Time	RMS	Time	RMS	Time
3	8.09e-04	0.018	6.09e-04	0.028	4.19e-04	0.088	3.09e-04	0.118
4	5.03e-04	0.018	3.03e-04	0.028	2.86e-04	0.085	2.01e-04	0.113
5	5.11e-04	0.021	4.11e-04	0.028	3.18e-04	0.085	4.11e-04	0.121
6	7.98e-04	0.026	5.98e-04	0.048	4.98e-04	0.108	3.98e-04	0.121
Average	6.55e-04	0.020	4.80e-04	0.096	3.80e-04	0.091	3.29e-04	0.118

Table 5 TDNN GDOP approximation results.

N. neuron	RMS	Time	RMS	Time	RMS	Time	RMS	Time
3	9.99e-04	0.012	5.59e-04	0.128	3.63e-04	0.188	2.09e-04	0.218
4	4.33e-04	0.012	2.68e-04	0.028	2.20e-04	0.035	1.86e-04	0.213
5	4.43e-04	0.012	3.11e-04	0.028	2.86e-04	0.045	4.11e-04	0.221
6	5.88e-04	0.021	4.98e-04	0.065	3.87e-04	0.118	3.98e-04	0.291
Average	6.15e-04	0.014	4.09e-04	0.062	3.14e-04	0.096	3.01e-04	0.235

Table 6 Compression TDNN method with other methods.

Method	TDNN	BP [12]	SVM [14]	GP [15]
Accuracy	99.48	91	98.40	99.60
Time Complexity	0.028	0.096	0.125	0.056

## 6 Conclusion

This paper is presented a study on the approximation and classification of GPS GDOP using TDNN. The TDNN is compared with other methods. The GPS GDOP approximation is a problem with nonlinear behavior. The experimental results show that this method has better performance than other methods. More accurate calculation of GDOP will increase the accuracy of low-cost GPS receiver. The TDNN-based GDOP approximation and classification is successfully conducted. The advantages of the TDNN network are summarized as follows: a simple local neural network that can treat as a lookup table, fast learning speed, high convergence rate, good generalization capability, and ease of implementation by hardware, etc. The experimental results show that the TDNN clustering for GDOP is highly effective. The average RMS error for a TDNN approximation is  $3.14e-04$  and the correct clustering percentage is more than 99%. This result indicates good clustering. The results demonstrate the superiority of the proposed algorithm with respect to the receiver internal algorithm.

## References

- [1] M. H. Refan, A. Dameshghi, and M. Kamarzarrin, "Improving RTDGPS accuracy using hybrid PSOSVM prediction model," *Aerospace Science and Technology*, Vol. 37, pp. 55–69, 2014.
- [2] M. H. Refan, A. Dameshghi, and M. Kamarzarrin, "Real-time differential global poisoning system stability and accuracy improvement by utilizing support vector machine," *International Journal of Wireless Information Networks*, Vol. 23, No. 1, pp. 66–81, 2016.
- [3] M. H. Refan, A. Dameshghi, and M. Kamarzarrin, "Utilizing hybrid recurrent neural network and genetic algorithm for predicting the pseudo-range correction factors to improve the accuracy of RTDGPS," *Gyroscope and Navigation*, Vol. 6, No. 3, pp. 197–206, 2015.
- [4] M. H. Refan, A. Dameshghi, and M. Kamarzarrin, "Implementing the reference and user stations of DGPS based on transmitting and applying RPCE factor," *Wireless Personal Communications*, Vol. 86, No. 4, pp.1–21, 2016.
- [5] M. H. Refan and A. Dameshghi, "Comparing error predictions of GPS position components using, ARMANN, RNN, and ENN in order to use in DGPS," in *20<sup>th</sup> Telecommunications Forum TELFOR*, Belgrad, SERBIA, pp. 815–818, 2012.
- [6] M. H. Refan, A. Dameshghi, and M. Kamarzarrin, "Using ME-PSO classification algorithm for clustering geometric dilution of precision," in *7<sup>th</sup> International Conference on e-Commerce in Developing Countries with Focus on e-Security*, Kish, Iran, 2013.
- [7] J. Zhang, J. Zhang, R. Grenfell, and R. Deakin, "GPS satellite velocity and acceleration determination using the broadcast ephemeris," *Journal of Navigation*, Vol. 59, pp. 293–305, 2006.
- [8] R. Yarlagadda, I. Ali, N. Al-Dhahir, and J. Hershey, "GPS GDOP metric," *IEEE Proceedings-Radar, Sonar and Navigation*, Vol. 147, No. 5, pp. 259–64, 2000.
- [9] S. Tafazoli and M. R. Mosavi, "Performance improvement of GPS GDOP approximation using recurrent wavelet neural network," *Journal of Geographic Information System*, Vol. 3, No. 4, pp. 318–322, 2001.
- [10] M. R. Mosavi and H. Azami, "Applying neural network for clustering of GPS satellites," *Journal of Geoinformatics*, Vol. 7, No. 3, pp. 7–14, 2011.
- [11] D. Simon and H. El-Sherief, "Navigation satellite selection using neural networks," *Neurocomputing*, Vol. 7, No. 2, pp. 47–58, 1995.
- [12] D. J. Jwo and K. P. Chin, "Applying back-propagation neural networks to GDOP approximation," *Journal Navigation*, Vol. 55, pp. 911–108, 2002.
- [13] D. J. Jwo and C. C. Lai, "Neural network-based GPS GDOP approximation and classification," *GPS Solutions*, Vol. 11, No. 1, pp. 51–60, 2007.
- [14] C. H. Wu, W. H. Su, and Y. W. Ho, "A study on GPS GDOP approximation using support vector machines," *IEEE Transactions on Instrumentation and Measurement*, Vol. 60, No. 1, pp. 137–45, 2011.
- [15] Ch. H. Wu, Y. W. Ho, L. W. Chen, and Y. D. Huang, "Discovering approximate expressions of GPS geometric dilution of precision using genetic programming," *Advances in Engineering Software*, Vol. 45, pp. 332–340, 2012.
- [16] H. Azami, M. R. Mosavi, and S. Sanei, "Classification of GPS satellites using improved back propagation training algorithms," *Wireless Personal Communications*, Vol. 71, No. 2, pp. 789–803, 2013.
- [17] M. Azarbad, H. Azami, S. Sanei, and A. Ebrahimzadeh, "New neural network-based approaches for GPS GDOP classification based on neuro-fuzzy inference system, radial basis function, and improved bee algorithm," *Applied Soft Computing*, Vol. 25, pp. 285–292, 2014.
- [18] L. Sheremetov, A. Cosultchi, J. Martínez-Muñoz, A. Gonzalez-Sánchez, and M. A. Jiménez-Aquino, "Data-driven forecasting of naturally fractured reservoirs based on nonlinear autoregressive neural networks with exogenous input," *Journal of Petroleum Science and Engineering*, Vol. 123, pp. 106–119, 2014.



- [19] N. Arasavali, S. Gottapu, and N. Kumar, "GDOP analysis with optimal satellites using GA for southern region of Indian subcontinent," *Procedia Computer Science*, Vol. 143, pp. 303–308, 2018.
- [20] Sh. Zhu, "An optimal satellite selection model of global navigation satellite system based on genetic algorithm," in *China Satellite Navigation Conference*, pp.585–595, May 2018.
- [21] Y. Teng, J. Wang, Q. Huang, and B. Liu, "New characteristics of weighted GDOP in multi-GNSS positioning," *GPS Solutions*, Vol. 22, pp.1–9, 2018.
- [22] E. Wang, Ch. Jia, T. Pang, P. Qu, and Zh. Zhang, "Research on BDS/GPS integrated navigation satellite selection algorithm based on particle swarm optimization," in *China Satellite Navigation Conference*, pp. 727–737, May 2018.
- [23] X. Liu, Sh. Zhang, Q. Zhang, N. Ding, and W. Yang, "A fast satellite selection algorithm with floating high cut-off elevation angle based on ADOP for instantaneous multi-GNSS single-frequency relative positioning," *Advances in Space Research*, Vol. 63, pp. 1234–1252, 2019.
- [24] Y. Shao and K. Nezu, "Prognosis of remaining bearing life using neural networks," *Proceedings of the Institution of Mechanical Engineers*, Vol. 214, No. 3, pp. 217–230, 2000.
- [25] A. Andalib and F. Atry, "Multi-step ahead forecasts for electricity prices using NARX: A new approach, a critical analysis of one-step ahead forecasts," *Energy Conversion and Management*, Vol. 50, No. 3, pp. 739–747, 2009.
- [26] H. Asgari, X. Chen, M. Morini, M. Pinelli, R. Sainudiin, P. R. Spina, and M. Venturini, "NARX models for simulation of the start-up operation of a single-shaft gas turbine," *Applied Thermal Engineering*, Vol. 93, pp. 368–376, 2015.
- [27] S. Çoruh, F. Geyikçi, E. Kılıç, and U. Çoruh, "The use of NARX neural network for modeling of adsorption of zinc ions using activated almond shell as a potential biosorbent," *Bioresource Technology*, Vol. 151, pp. 406–410, 2014.
- [28] M. Ardalani-Farsa and S. Zolfaghari, "Chaotic time series prediction with residual analysis method using hybrid Elman–NARX neural networks," *Neurocomputing*, Vol. 73, No. 13, pp. 2540–2553, 2010.
- [29] W. Huang, Ch. Yan, J. Wang, and W. Wang, "A time-delay neural network for solving time-dependent shortest path problem," *Neural Networks*, Vol. 90, pp. 21–28, 2017.
- [30] U-blox 6 receiver description including protocol specification, [Online]. Available: <http://www.u-blox.com/en/gps-modules.html>.



**M. H. Refan** received his B.Sc. in Electronics Engineering from Iran University of Science and Technology (IUST), Tehran, Iran in 1972. After 12 years of working and experience in the industry, he started studying again in 1989 and received his M.Sc. and Ph.D. in the same field and the same University in 1992 and 1999 respectively. He is currently an Associated Professor of Electrical Engineering Faculty, Shahid Rajaei Teacher Training University (SRTTU), Tehran, Iran. He is author of about 50 scientific publications on journals and international conferences. His research interests include GPS, DCS, and automation systems.



**A. Dameshghi** was born in 1986 and received his B.Sc. and M.Sc. degrees in Electronic Engineering from the Department of Electrical Engineering, of Electrical Engineering, Shahid Rajaei Teacher Training University (SRTTU), Tehran, Iran, in 2011 and 2013, respectively. He is currently a Ph.D. candidate at SRTTU. His research interests include boolean function, global positioning systems, electric and hybrid vehicles.



© 2020 by the authors. Licensee IUST, Tehran, Iran. This article is an open access article distributed under the terms and conditions of the Creative Commons Attribution-NonCommercial 4.0 International (CC BY-NC 4.0) license (<https://creativecommons.org/licenses/by-nc/4.0/>).